Efficient Luminescence from Easily Prepared Three-Coordinate Copper(I) Arylamidophosphines

Kenneth J. Lotito and Jonas C. Peters
Department of Chemistry, Massachusetts Institute of Technology,
Cambridge, MA 02139

Supporting Information

Experimental Section

General Considerations. All manipulations were carried out under a dinitrogen atmosphere using standard glovebox techniques. All solvents were deoxygenated and dried by sparging with Ar followed by passage through an activated alumina column from S.G. Water (Nashua, N.H.) Solvents were tested with a standard purple solution of benzophenone ketyl in THF to confirm effective oxygen and moisture removal. Methylcyclohexane and cyclopentane were of spectroscopic grade. Deuterated solvents were purchased from Cambridge Isotope Laboratories, Inc., were degassed, and stored over 3 Å molecular sieves prior to use. Bis-(4-fluorophenyl)[1] amine and mesityl copper(I)[2] were prepared according to literature procedures. Lithium amides were prepared from the Et_2O or THF solutions of the corresponding aryl amines by treatment with a hexane solution of n-butyllithium at -78 °C. The stoichiometry of coordinated solvent molecules in the lithium reagents was estimated from ^{1}H NMR spectroscopy. Celite (Celite® 545) was dried at 300 °C under vacuum for 48 hours. Glass microfiber filters were dried prior to use by heating at 350 °C for 48 hours. All other starting reagents and materials were obtained from commercial vendors and used without further purification. Elemental analyses were performed by Midwest Microlabs (Indianapolis Indiana). NMR spectra were recorded at ambient temperature on Bruker Avance 400 MHz spectrophotometers. ^{1}H and ^{13}C NMR spectra are referenced to residual solvent. ^{31}P NMR spectra are reported relative to an external standard of 85% H_3PO_4 (δ = 0 ppm). ^{19}F NMR spectra are reported relative to an external standard of C_6F_6 (δ = -164.9 ppm) or C_6H_5F (δ = -113.15 ppm). UV-Vis absorption measurements were recorded on a Varian Cary 50 UV-Vis spectrophotometer using 1 cm path length quartz cuvettes equipped with an air-tight screw cap.

Electrochemistry. Electrochemical measurements were carried out in a glovebox under a dinitrogen atmosphere in a single-compartment cell using a BAS model 100/W electrochemical analyzer. A freshly polished glassy carbon electrode and a coiled platinum wire were used as the working and auxiliary electrodes, respectively. The reference electrode was $Ag/AgNO_3$ in THF. Samples were prepared by dissolving a small quantity (ca. 3 mg) of analyte in approximately 3 mL of a 0.3 M $[(Bu)_4N][PF_6]$ electrolyte solution in THF. The reference electrode was calibrated before and after measurements using an external ferrocene standard.

X-ray Crystallography Procedures. X-ray quality crystals were grown as indicated in the experimental section. Single crystals were mounted on a glass fiber using Paratone-N oil. Low-temperature single-crystal diffraction studies were collected on a Siemens Platform three-circle diffractometer coupled to a Bruker-AXS Smart Apex CCD detector with graphite monochromated Mo Kα radiation (λ= 0.71073) performing φ- and ω-scans. The structure was solved by the Patterson method using SHELXS[3] and refined against F^2 on all data by full-matrix least squares with SHELXL-97.[4] All non-hydrogen atoms were refined anisotropically. Hydrogen atoms were included at the model at geometrically calculated positions and refined using a standard riding model. The isotropic displacement parameters of the hydrogen atoms were fixed to 1.2 times the *U* values of the atoms they are linked to (1.5 times for methyl groups).

The diffraction data for $(PPh_3)_2Cu(NTol_2)$ (**2**) exhibited characteristic features of non-merohedral twinning and was refined accordingly:[5] Two crystallographically independent domains with identical unit cell parameters were identified from the diffraction pattern using the Cell_Now[6] software included in the SHELX package. The domains were present in approximately a 60:40 ratio. The twinned data set was reduced in SAINT and absorption correction performed using TWINABS. The reflection data was written into the multi-domain HKL5 file format. At this point, the structure was refined by standard methods.

A single phenyl substituent of the diphenylamide ligand in $(PPh_3)_2Cu(NPh_2)$ (**1**) was disordered over two positions with 75:25 relative occupancy. The disorder was incorporated in the final model. The unit cell also contained two half-benzene molecules located on inversion centers. The refinement of these moieties was facilitated by the use of similarity restraints on the 1,2- and 1,3-distances.

Luminescence Lifetime Measurements. Analyte solutions were prepared in a nitrogen-filled glovebox by suspending a small amount (ca. 2 mg) of copper complex in ca. 20 mL of MeCy, in which they were sparingly soluble. The saturated solutions were then filtered through a glass microfiber filter into quartz fluorescence cuvettes (1 cm path length), the concentrations adjusted with additional filtered MeCy, fit with an air-tight screw cap, and brought out of the glovebox. The concentration of analyte in each sample was 1 x 10^{-4} M or below. Luminescence lifetimes were determined by time-resolved phosphorescence spectroscopy as previously described.[7] The irradiation source was an Oriel nitrogen laser (Model 79111) with a 5 ns pulse width operating at approximately 3 Hz. The emitted light was dispersed in an Oriel MS-260i spectrograph with a 300 lines/mm grating and was detected by an Andor Technologies Intensified CCD camera (1024 x 128 pixels) with an onboard delay generator and a minimum gate width of 5 ns, operating in full vertical binning mode and triggered by a TTL pre-pulse from the nitrogen laser. The detector was calibrated using an Hg(Ar) pen lamp. Measurements were performed at ambient temperature. Measured values at each gate step position were accumulated from 15 pulses. All kinetic traces exhibited monoexponential decay and were fit to a first-order model. Decay constants for each sample were determined at three wavelengths at and around the emission maximum and averaged. The reported value is the average obtained from at least 2 samples.

Table S1. Data for Luminescence Lifetime Measurements.

Compound	O. D. at 337 nm	k_{obs} (μs^{-1})	Lifetime (τ) (μs)
1	1.422 0.549 0.200	0.3206 0.3152 0.3116	3.1 3.2 3.2 3.15(5) (avg.)
2	0.748 0.270 0.099	0.3372 0.3096 0.3087	3.0 3.2 3.2 3.1(2) (avg.)
3	0.532 0.152 0.066 0.099	0.4022 0.3955 0.4085 0.3715	2.5 2.5 2.4 2.7 2.5(1) (avg.)
4	1.124 1.089	0.3870 0.4030	2.58 2.48 2.5(1) (avg).
5	0.665 0.659	0.3707 0.3673	2.70 2.72 2.71(2) (avg.)
6	0.873 0.411	0.5855 0.5892	1.71 1.69 1.70(1) (avg.)

7	0.036	0.0901	11.1
	0.022	0.0801	12.3
	0.016	0.0851	11.7
			11.7(6) (avg.)

Quantum Yield Measurements. Analyte solutions were prepared in a nitrogen-filled glovebox by suspending a small amount (ca. 2 mg) of copper complex in ca. 20 mL of MeCy, in which they were sparingly soluble. The saturated solutions were then filtered through a glass microfiber filter into quartz fluorescence cuvettes (1 cm path length), the concentrations adjusted by the addition of MeCy, fit with an air-tight screw cap and brought out of the glovebox. The concentration of analyte in each sample was 1 x 10^{-4} M or below. Emission spectra were collected on a SPEX Fluorolog-τ3 fluorimeter (Model FL-321, 450 W xenon lamp) using right angle detection. The optical density of each sample was kept near or below 0.1 at the wavelength of excitation and at longer wavelengths to minimize reabsorption of emitted light. Luminescence measurements were performed using a 390 nm excitation at 298 K. Excitation monochrometer slits were adjusted to allow for 3 nm resolution while the emission monochrometer slits were adjusted to allow for 5 nm resolution. Quantum yields were calculated from the measured quantities by the method of Demas and Crosby.[8] All quantum yields are reported in reference to a standard sample of perylene in benzene with a reported quantum yield value of $\Phi_R = 0.99$.[9] The reported value is the average of at least two samples. The complete emission data is provided in **Table S2**.

Table S2. Data for Quantum Yield Measurements in MeCy at 298 K

Complex	**λ_{ex} (nm)**	**O.D. at 390 nm**	**I (counts)**[a]	**Φ (calc.)**[c]
(standard)	390	0.065	9.958 x 10^9	
1		0.100	4.441 x 10^9	0.26
1		0.113	5.031 x 10^9	0.26
(standard)	390	0.027	6.644 x 10^9	
1		0.069	3.495 x 10^9	0.18
(standard)	390	0.041	1.446 x 10^{10}	
2		0.132	1.137 x 10^{10}	0.23
2		0.069	6.319 x 10^9	0.22
(standard)	390	0.028	6.773 x 10^9	
3		0.097	3.043 x 10^9	0.12
3		0.136	4.038 x 10^9	0.11
(standard)	390	0.100	1.022 x 10^{10}	
3		0.009	1.916 x 10^8	0.18
3		0.019	2.431 x 10^8	0.11
4	390	0.094	2.558 x 10^9	0.16
4		0.134	3.366 x 10^9	0.15
(standard)			6.748 x 10^9	
4	390	0.080	6.663 x 10^9	0.12
4		0.084	7.028 x 10^9	0.12
4		0.083	7.205 x 10^9	0.12
(standard)			1.477 x 10^9	
5[b]	390	0.126	3.330 x 10^9	0.11
5[b]		0.144	3.982 x 10^9	0.11
5[b]		0.058	1.596 x 10^9	0.11

(standard)		0.051	1.096×10^{10}	
6	390	0.040	1.580×10^{9}	0.19
6		0.025	9.188×10^{8}	0.18
(standard)		0.029	5.380×10^{9}	
7	390	0.010	6.335×10^{8}	0.22
7		0.009	1.432×10^{9}	0.27
(standard)		0.016	2.889×10^{9}	

a. Integrated luminescence intensity.
b. In C_5H_{10}.
c. Uncertainty in quantum yield values is estimated at ± 0.05.

Computational Details. DFT calculations were performed on $(PPh_3)_2Cu(N(p\text{-}Tol)_2)$ **(2)** using the Gaussian 03 program package.[10] Molecular orbitals and energies were determined from a single-point calculation using the B3LYP hybrid functional[11] and the 6-31+G*[12] basis set. Input coordinates were obtained from the solid-state structure.

Synthesis of $(Ph_3P)_2Cu(NPh_2)$ (1), Method A. A solution of triphenylphosphine (255 mg, 0.97mmol, 2 eq.) in 3 ml benzene was added to a stirring suspension of $CuBr \cdot SMe_2$ (100 mg, 0.49 mmol, 1 eq.) in 3 ml benzene causing the suspended solids to dissolve. $Li(NPh_2) \cdot 1.33\ Et_2O$ (133 mg, 0.49 mmol, 1 eq.) was added in portions as a suspension in 3 ml benzene to the stirring copper-phosphine mixture causing the immediate production of a bright green luminescence. The solution was stirred at ambient temperature for 5 h then concentrated *in vacuo* to a volume of 2 mL. The concentrated solution was passed through a glass microfiber filter packed with Celite. The filter was extracted with benzene until the total volume of the filtered solution was 5 mL. The solution was carefully layered with 15 mL *n*-pentane and allowed to stand undisturbed for 3 days after which large green-yellow crystalline blocks and needles had grown. The solution was cooled to -30 °C for 2 hr then filtered. The solids were rinsed once with *n*-pentane and briefly dried *in vacuo*. Yield: 312 mg (85%). ^{1}H NMR (C_6D_6, 400 MHz): δ 7.50 (d, 4H, NAr-*H*), 7.35 (t, 12H, $P(C_6H_5)_3$), 7.13 (t, 4H, NAr-*H*), 7.00 – 6.88 (m, 18H, $P(C_6H_5)_3$), 6.70 (t, 2H, NAr-*H*). $^{31}P\{^1H\}$ NMR (C_6D_6, 162 MHz): δ -2.01 (br). $^{13}C\{^1H\}$ NMR (C_6D_6, 100 MHz): δ 134.20 (d, J_{PC} = 15.4 Hz), 129.80, 129.41, 128.91 (d, J_{PC} = 8.9 Hz), 120.89, 116.42. Anal. calcd. for $C_{50}H_{44}CuNP_2$ C, 76.56; H, 5.65; N, 1.79; Found: C, 76.23; H, 5.65; N, 1.89.

Synthesis of $(Ph_3P)_2Cu(NPh_2)$ (1), Method B. A solution of triphenylphosphine (72 mg, 0.27 mmol, 2 eq.) in 3 mL benzene was added to a stirring solution of mesityl copper (25 mg, 0.14 mmol, 1 eq.) in 3 mL benzene causing the yellow solution to lighten slightly. After stirring for ca. 5 minutes, diphenylamine (23 mg, 0.14 mmol, 1 eq.) in 3 mL benzene was added to the stirring copper-phosphine mixture. After stirring for 3-days at room temperature, a bright green luminescent solution had developed. The solvent was concentrated *in vacuo* to a volume of 2 mL, filtered through a glass microfiber filter packed with Celite. 10 mL n-pentane was added and the solution cooled to -30 °C overnight, affording a bright green microcrystalline solid. The solid was filtered, rinsed with n-pentane, and dried briefly *in vacuo*. Yield: 22 mg (19%). Spectroscopic data were identical to that of the material obtained by method A.

Synthesis of $(Ph_3P)_2Cu(NTol_2)$ (2). 2 was synthesized by the same procedure as **1** method A, except $Li(N(p\text{-}FPh)_2) \cdot 0.66\ Et_2O$ (127 mg, 0.49 mmol, 1 eq.) was used instead of $Li(NPh_2) \cdot 1.33\ Et_2O$. Analytically pure material was obtained by cooling a solution of **2** in 20 mL of a 3:2 v/v mixture of

n-pentane and benzene at -30 °C for 2 days. Yield: 258 mg (68 %). Crystals satisfactory for X-ray diffraction analysis were obtained by layering a concentrated solution of **2** in benzene with pentane, giving translucent yellow blocks overnight. ^{1}H NMR (C_6D_6, 400 MHz): δ 7.44 (d, 4H, NAr-*H*), 7.35 (t, 12H, P(C_6H_5)$_3$), 6.90 – 7.01 (m, 22H, NAr-*H* and P(C_6H_5)$_3$), 2.23 (s, 6H, Ar-CH_3). ^{31}P{^{1}H} NMR (C_6D_6, 162 MHz): δ -2.01 (br). ^{13}C{^{1}H} NMR (C_6D_6, 100 MHz): δ 134.25 (d, J_{PC} = 16.1 Hz), 130.02, 129.65, 128.87 (d, J_{PC} = 8.7 Hz). Anal. calcd. for $C_{58}H_{40}CuNP_2$ C, 76.22; H, 5.33; N, 1.85; Found: C, 75.97; H, 5.40; N, 1.87.

Synthesis of (Ph_3P)$_2$Cu(N(*p*-FPh)$_2$) (3). 3 was synthesized by the same procedure as **1** method A, except Li(N(*p*-FPh)$_2$) ·0.66 Et_2O (127 mg, 0.49 mmol, 1 eq.) was used instead of Li(NPh_2) ·1.33 Et_2O. Crystals of **3** were grown by layering a benzene solution of the complex with pentane, giving small, bright yellow, microcrystalline fibers after 3 days. Yield: 351 mg (91%). Analytically pure material was obtained by an additional recrystallization from benzene/pentane. Crystals suitable for X-ray diffraction were obtained by layering a 5 mL of a non-saturated solution of **3** with 15 mL pentane. Thick brown needles were obtained after 3 days. ^{1}H NMR (C_6D_6, 400 MHz): δ 7.30 (t, 12H, P(C_6H_5)$_3$), 7.14 (d, 4H, NAr-*H*), 7.00 – 6.86 (m, 18H, P(C_6H_5)$_3$), 6.77 (s, 4H, NAr-*H*). ^{31}P{^{1}H} NMR (C_6D_6, 162 MHz): δ -2.80 (br). ^{19}F NMR (C_6D_6, 376 MHz): δ -128.05. ^{13}C{^{1}H} NMR (C_6D_6, 100 MHz): δ 134.13 (d, J_{PC} = 15.3 Hz), 133.79, 133.53, 129.92, 128.94 (d, J_{PC} = 8.9 Hz), 120.92, 115.71 (d, J_{PC} = 21.3 Hz). A satisfactory elemental analysis could not be obtained for **3**, but the ^{1}H, ^{31}P, and ^{19}F NMR spectra of spectroscopically pure material is provided in Figure S1.

Synthesis of ((*p*-Tol)$_3$P)$_2$Cu(NPh_2) (4). 4 was synthesized by the same procedure as **1** method A, except P(*p*-Tol)$_3$ (148 mg, 0.49 mmol, 2 eq.) was used instead of triphenylphosphine. Analytically pure crystals of **4** were obtained by layering a saturated benzene solution with pentane. Yield: 136 mg (67 %). ^{1}H NMR (C_6D_6, 400 MHz): δ 7.61 (d, 4 H, NAr-*H*), 7.42 (t, 12 H, P(C_6H_5)$_3$), 7.21 (t, 4 H, NAr-*H*), 6.82 (d, 12 H, P(C_6H_5)$_3$), 6.73 (t, 2 H, NAr-*H*), 1.96 (s, 18 H, -CH_3). ^{31}P{^{1}H} NMR (C_6D_6, 162 MHz): δ -4.40. ^{13}C{^{1}H} NMR (C_6D_6, 100 MHz): δ 157.26, 140.16, 134.60 (d, J_{PC} = 15.4 Hz), 130.06 (d, J_{PC} = 9.4 Hz), 127.78, 121.20, 116.61, 21.50. Anal. calcd. for $C_{54}H_{52}CuNP_2$ C, 77.17; H, 6.24; N, 1.67; Found: C, 76.80; H, 6.12 N, 1.53.

Synthesis of ((*p*-FPh)$_3$P)$_2$Cu(NPh_2) (5). 5 was synthesized by the same procedure as **1** method A, except P(*p*-FPh)$_3$ (196 mg, 0.53 mmol, 2 eq.) was used instead of triphenylphosphine. **5** was obtained as an analytically pure yellow solid by layering a saturated benzene solution with pentane producing crystalline material of varying morphology after 2 days. Yield: 160 mg (76 %). ^{1}H NMR (C_6D_6, 400 MHz): δ 7.31 (d, 4 H, NAr-*H*), 7.08 - 6.97 (m, 16 H, NAr-*H* and P(C_6H_5)$_3$), 6.67 (t, 2 H, NAr-*H*), 6.63 (t, 12 H, P(C_6H_5)$_3$). ^{31}P{^{1}H} NMR (C_6D_6, 162 MHz): δ -5.58. ^{19}F NMR (C_6D_6, 376 MHz): δ -109.71. ^{13}C{^{1}H} NMR (C_6D_6, 100 MHz): δ 165.80, 163.29, 157.03, 136.28 (dd, J_{PC} = 17.5, Hz, J_{PC} = 8.2 Hz), 129.86, 121.67, 116.62 (dd, J_{PC} = 21.1, J_{PC} = 9.8). Anal. calcd. for $C_{48}H_{34}CuF_6NP_2$ C, 66.70; H, 3.97; N, 1.62; Found: C, 66.46; H, 3.89; N, 1.29.

Synthesis of (DPEPhos)Cu(NPh_2) (6). 6 was synthesized by the same procedure as **1** method A, except 1 eq. DPEphos (262.0 mg, 0.49 mmol, 1 eq.) was used instead of 2 eq. triphenylphosphine. **6** was obtained as a bright yellow microcrystalline solid by layering a saturated benzene solution of the complex with pentane. Yield: 251 mg (67%). Analytically pure material was obtained by an additional recrystallization as described above. ^{1}H NMR (C_6D_6, 400 MHz): δ 7.58 (d, 4 H, NAr-*H*), 7.33 (s, 8 H, P(C_6H_5)$_2$), 7.06 (t, 4 H, NAr-*H*), 6.94 (t, 12 H, P(C_6H_5)$_2$), 6.82 – 6.72 (m, 4 H, -C_6H_4-O-C_6H_4-), 6.67, (t, 2 H, C_6H_4-O-C_6H_4-), 6.58 (d, 2 H, C_6H_4-O-C_6H_4-), 6.49 (t, 2H, NAr-*H*). ^{31}P{^{1}H} NMR (C_6D_6, 162 MHz): δ -18.67. ^{13}C{^{1}H} NMR (C_6D_6, 100 MHz): δ 157.97, 134.88, 134.75 (d, J_{PC} = 8.8

Hz), 131.35, 130.22, 121.11, 116.11. Anal. calcd. for $C_{48}H_{38}CuNOP_2$ C, 74.84; H, 4.97; N, 1.82; Found: C, 74.95; H, 5.16; N, 1.54.

Synthesis of $(Ph_3P)_2Cu$(carbazolate) (7). **7** was synthesized by the same procedure as **1** method A, except Li(carbazolate) ·2.25 THF (81.6 mg, 0.24 mmol, 1 eq.) was used instead of $Li(NPh_2)$ ·1.33 Et_2O. Large, pale yellow, analytically pure crystals of **7** were obtained by layering a benzene solution with n-pentane. Yield: 121 mg (64 %). ^{1}H NMR (C_6D_6, 400 MHz): δ 8.52 (d, 2H, NAr-*H*), 7.67 ((d, 2H, NAr-*H*), 7.38 (t, 2H, NAr-*H*), 7.35 – 7.25 (m, 14H, NAr-*H* and $P(C_6H_5)_3$), 6.91 (t, 6H, $P(C_6H_5)_3$), 6.81 12H, $P(C_6H_5)_3$). $^{31}P\{^1H\}$ NMR (C_6D_6, 162 MHz): δ -2.85 (br). $^{13}C\{^1H\}$ NMR (C_6D_6, 100 MHz): δ 151.30, 134.13 (d, J_{PC} = 15.1 Hz), 130.07, 129.04 (J_{PC} = 9.0 Hz), 123.84, 120.53, 115.71, 115.09. Anal. calcd. for $C_{50}H_{44}CuNP_2$ C, 76.56; H, 5.65; N, 1.79; Found: C, 76.23; H, 5.65; N, 1.89.

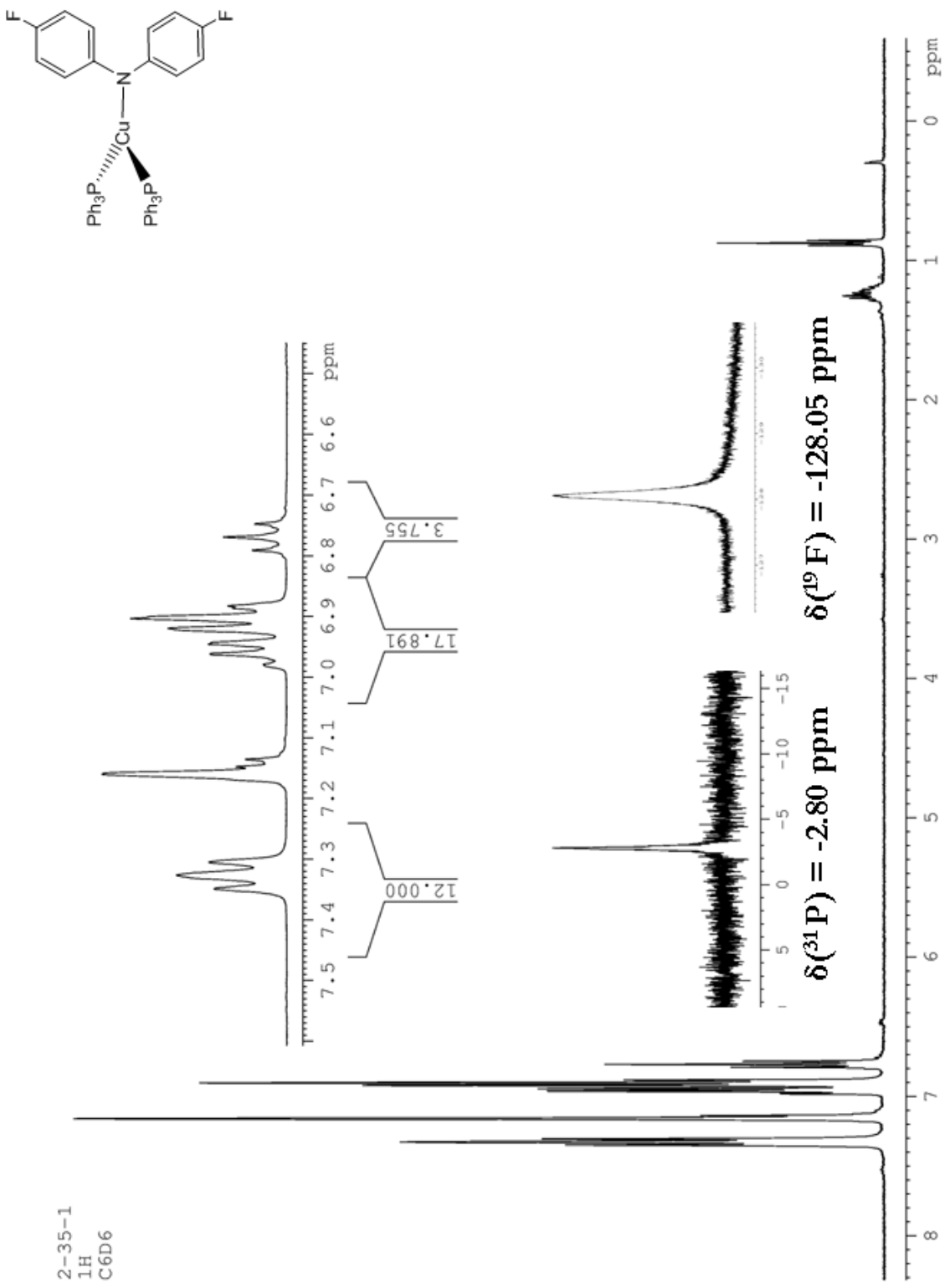

Figure S1. ^{1}H, ^{31}P, and ^{19}F NMR spectra of $(Ph_3P)_2Cu(N(p\text{-}FPh)_2)$ (**3**).

Table S3. Electrochemical properties of complexes measured by cyclic voltammetry.[a,b]

Compound	Type	E_{pa} (V)	E_{pc} (V)	$E_{1/2}$ (V)
1	Irreversible	0.590	-	-
2	Reversible	0.458	0.374	0.416
3	Irreversible	0.620	-	-
4	Irreversible	0.575	-	-
5	Irreversible	0.590	-	-
6	Irreversible	0.568	-	-
7	Irreversible	0.091	-	-

a. All measurements made at a scan rate of 100 mV/s.
b. All potentials reported relative to a Fc/Fc^+ external standard.

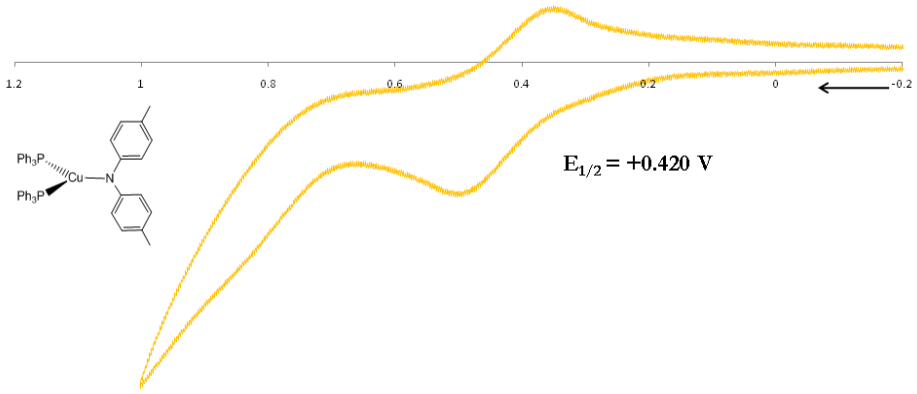

Figure S2. Cyclic voltammagram of **2** in 0.3 M $TBAPF_6$ electrolyte solution in THF. Potentials are reported relative to Fc/Fc^+. The scan rate is 100 mV/s.

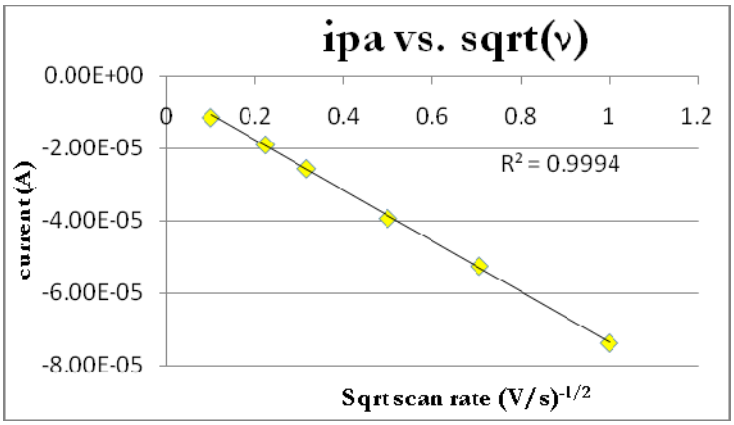

Figure S3. Dependence of i_{pa} on the square root of the scan rate for $(Ph_3P)_2Cu(NTol_2)$ (**2**).

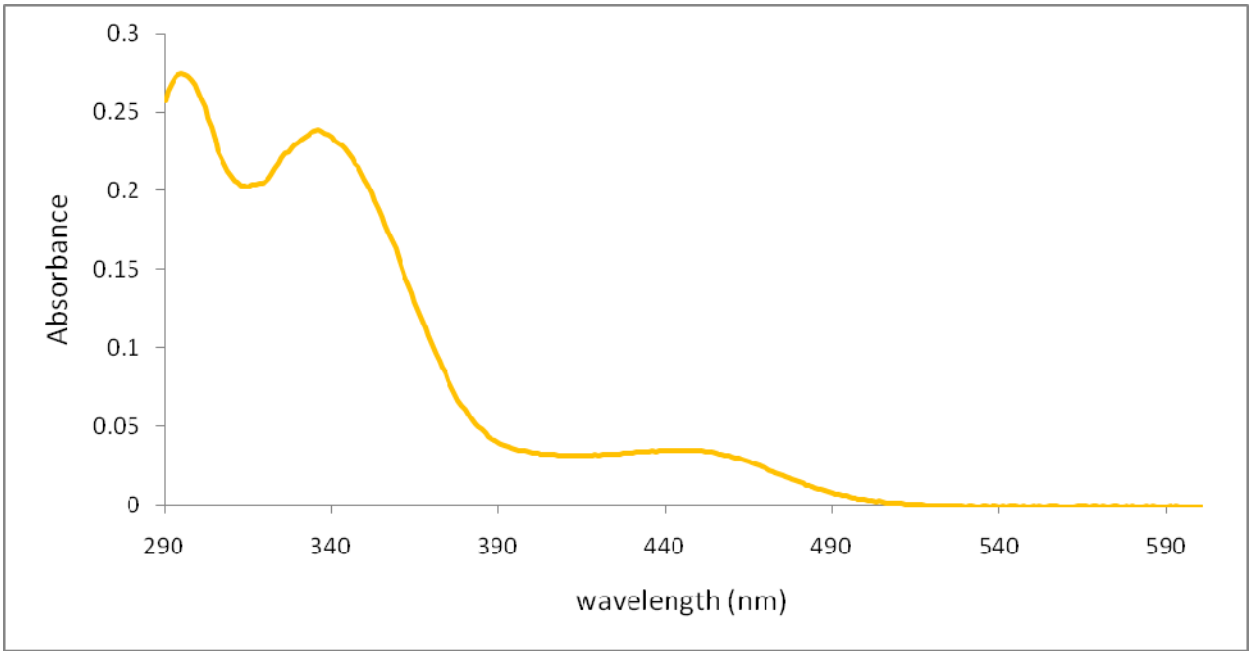

Figure S4. Absorption spectrum of (DPEphos)Cu(NPh_2) in MeCy. (**6**).

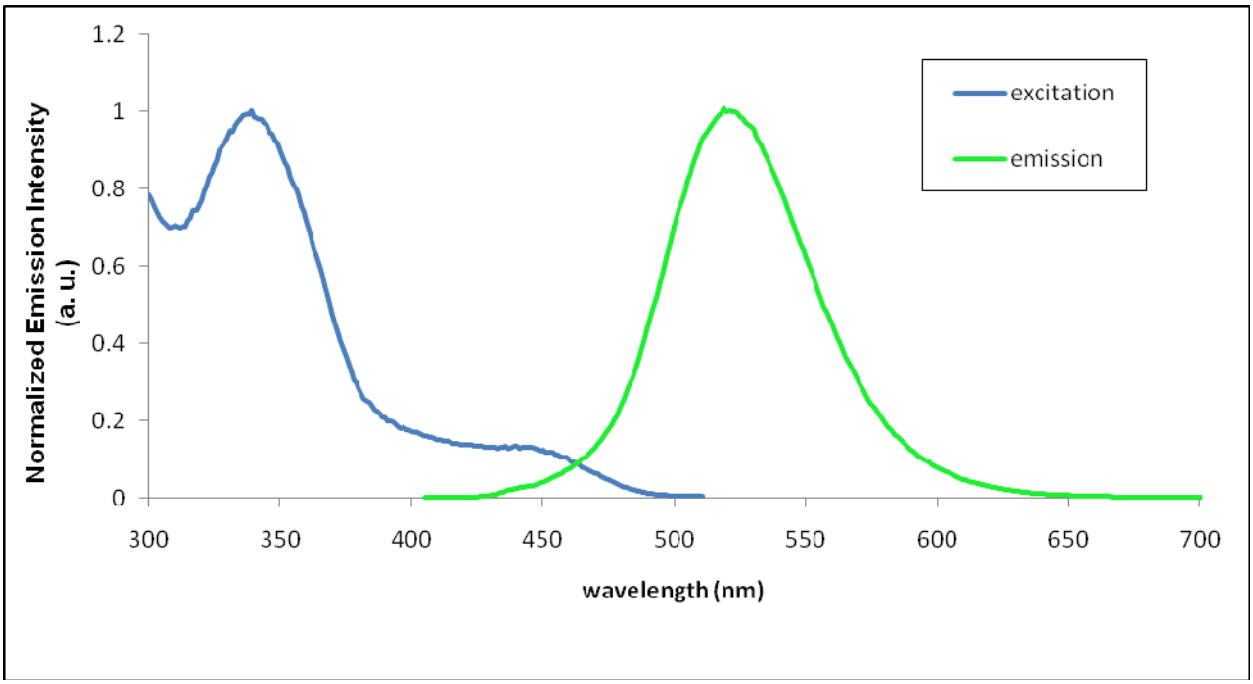

Figure S5. Excitation and emission spectra of $(Ph_3P)_2Cu(NPh_2)$ (**1**, λ_{ex} = 390 nm, λ_{em} = 521 nm).

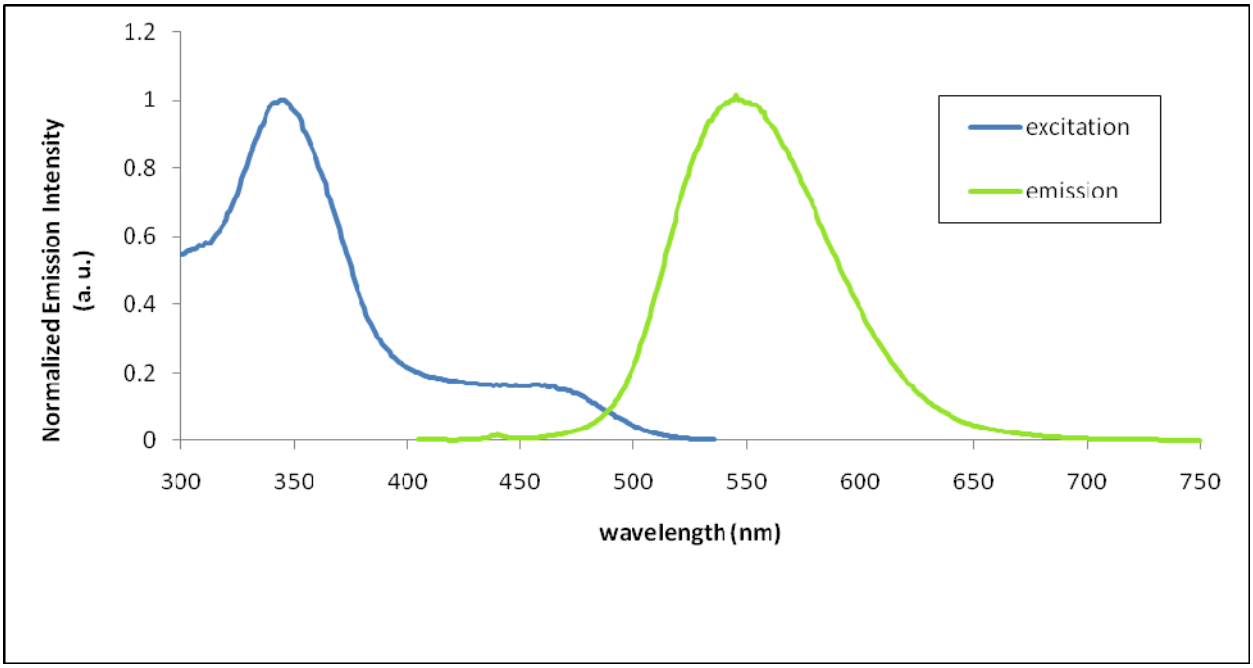

Figure S6. Excitation and Emission Spectra of $(Ph_3P)_2Cu(NTol_2)$ (**2**, λ_{ex} = 390 nm, λ_{em} = 546 nm).

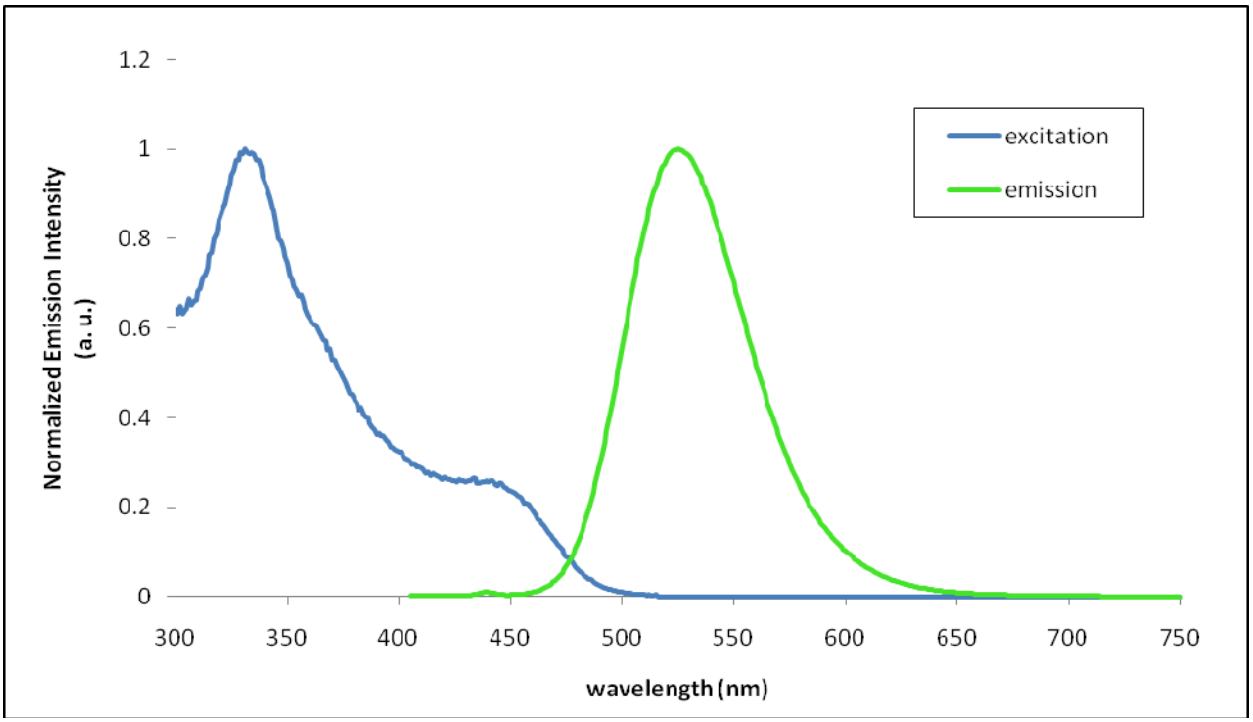

Figure S7. Excitation and emission spectrum of $(Ph_3P)_2Cu(N(p\text{-}FPh)_2)$ (**3**, λ_{ex} = 390 nm, λ_{em} = 525 nm).

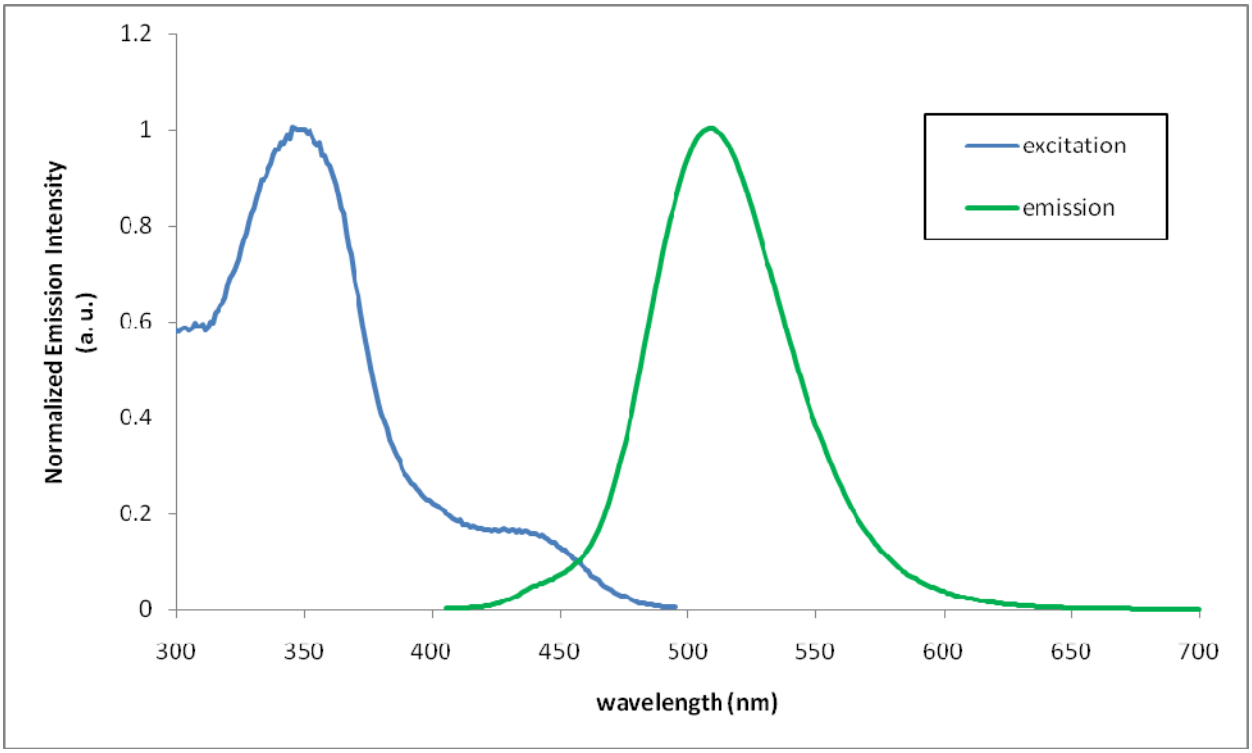

Figure S8. Excitation and emission spectra of $(PTol_3)_2Cu(NPh_2)$ (**4**, λ_{ex} = 390 nm, λ_{em} = 509 nm).

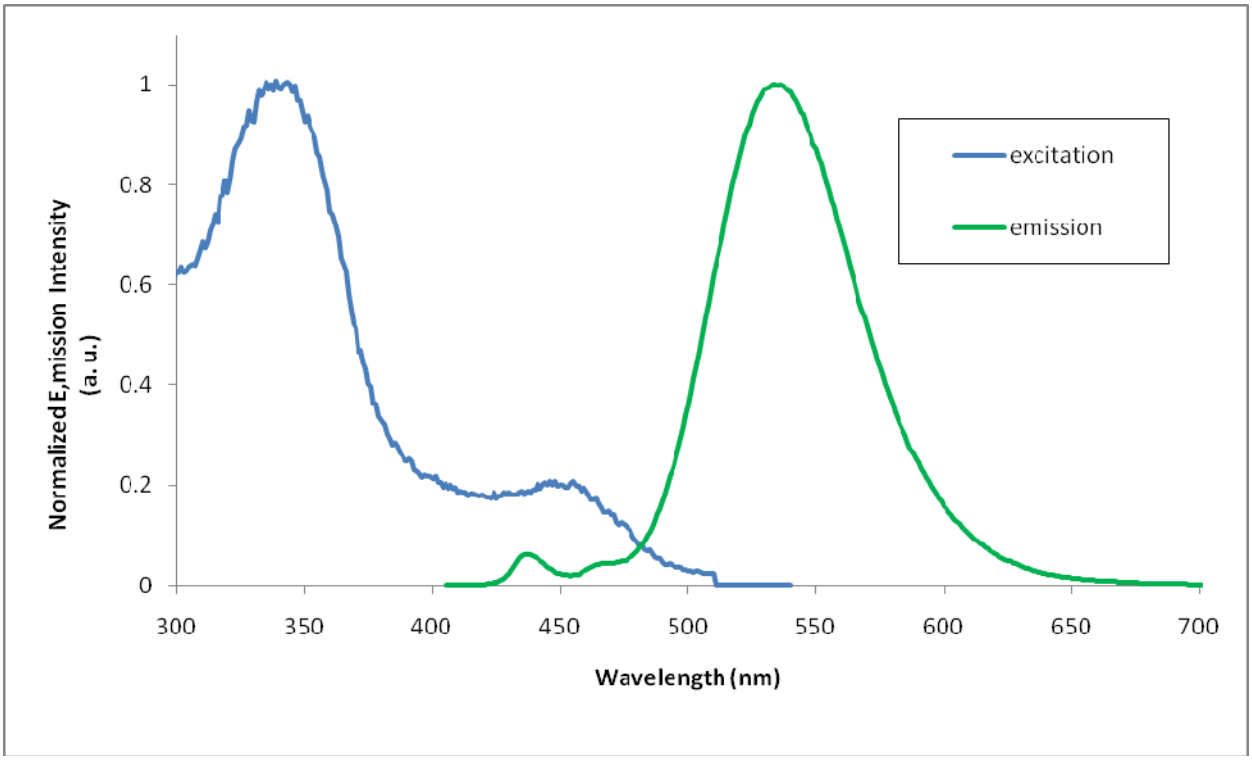

Figure S9. Excitation and emission spectra of $(P(p\text{-}FPh)_3)_2Cu(NPh_2)$ (**5**, λ_{ex} = 390 nm, λ_{em} = 535 nm).

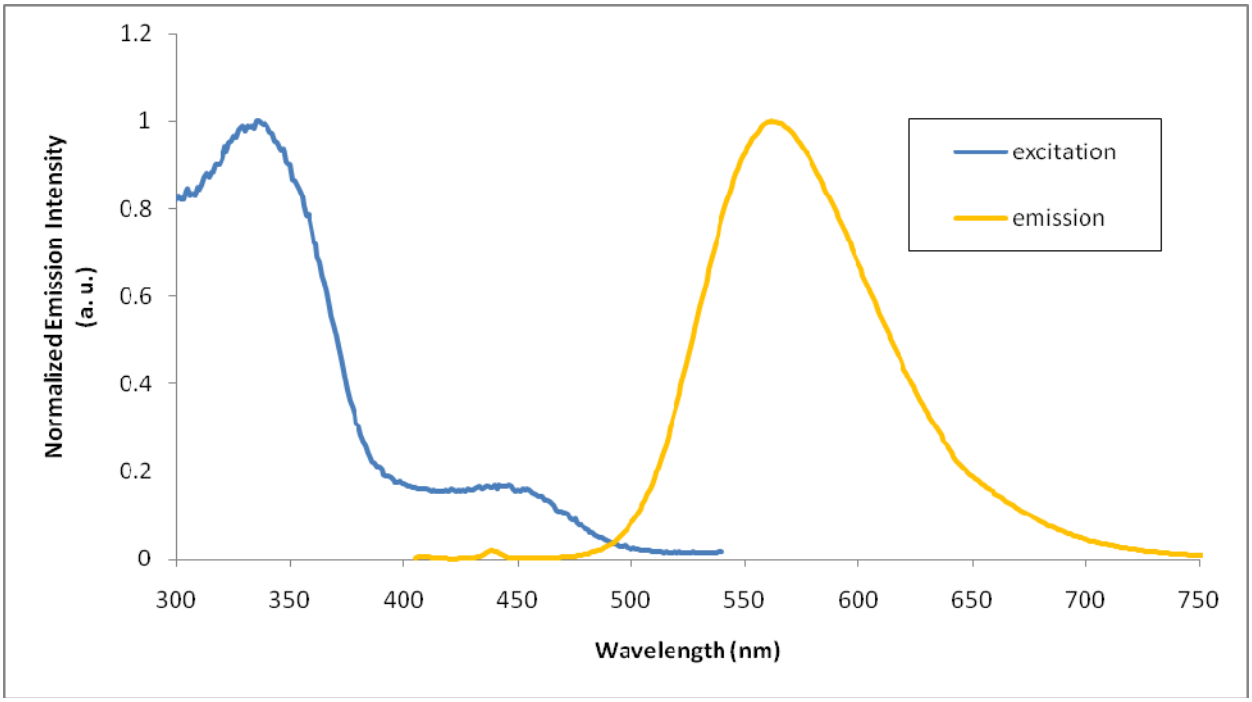

Figure S10. Excitation and emission spectra of $(DPEphos)_2Cu(NPh_2)$ (**6**, λ_{ex} = 390 nm, λ_{em} = 562 nm).

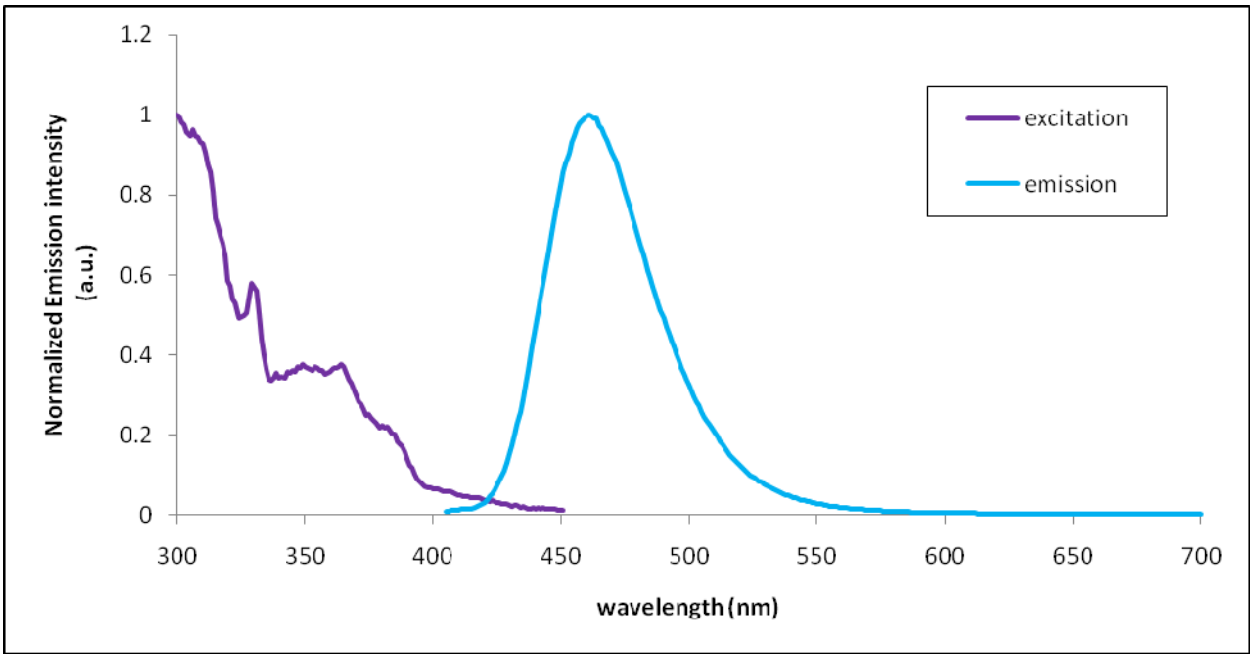

Figure S11. Excitation and emission spectra of $(Ph_3P)_2Cu(cbz)$ (**7**, λ_{ex} = 390 nm, λ_{em} = 461 nm).

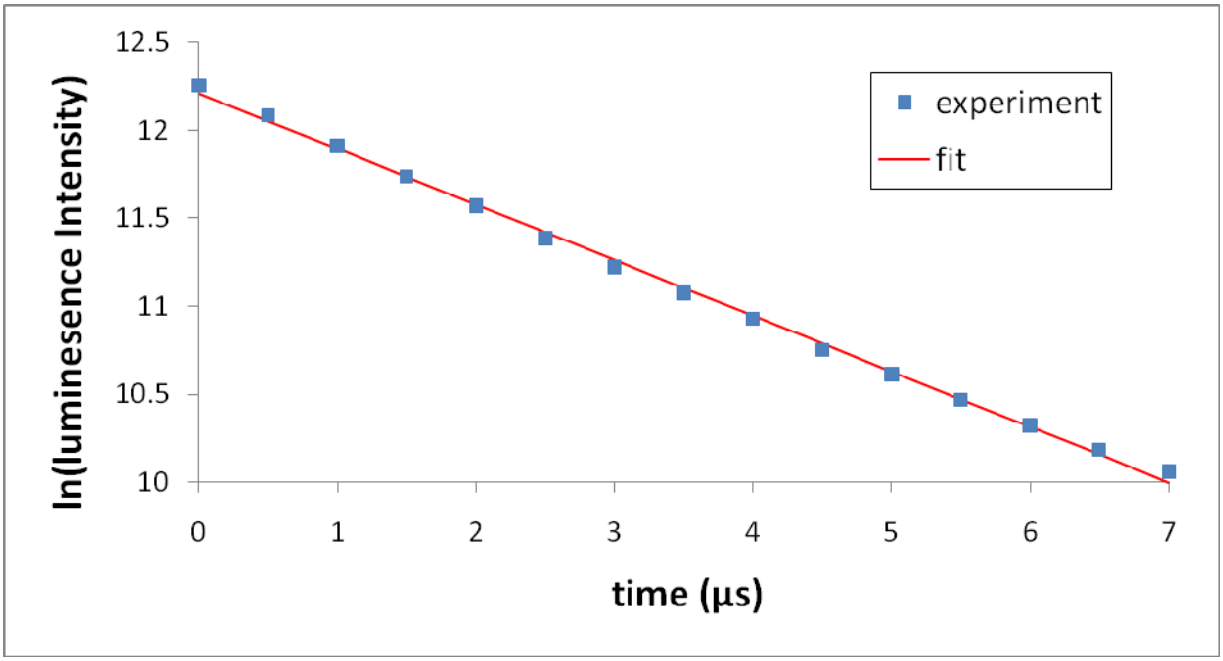

Figure S12. Luminescence decay trace of $(Ph_3P)_2Cu(NPh_2)$ (**1**, λ_{ex} = 337 nm, λ_{em} = 521 nm) with monoexponential fit.

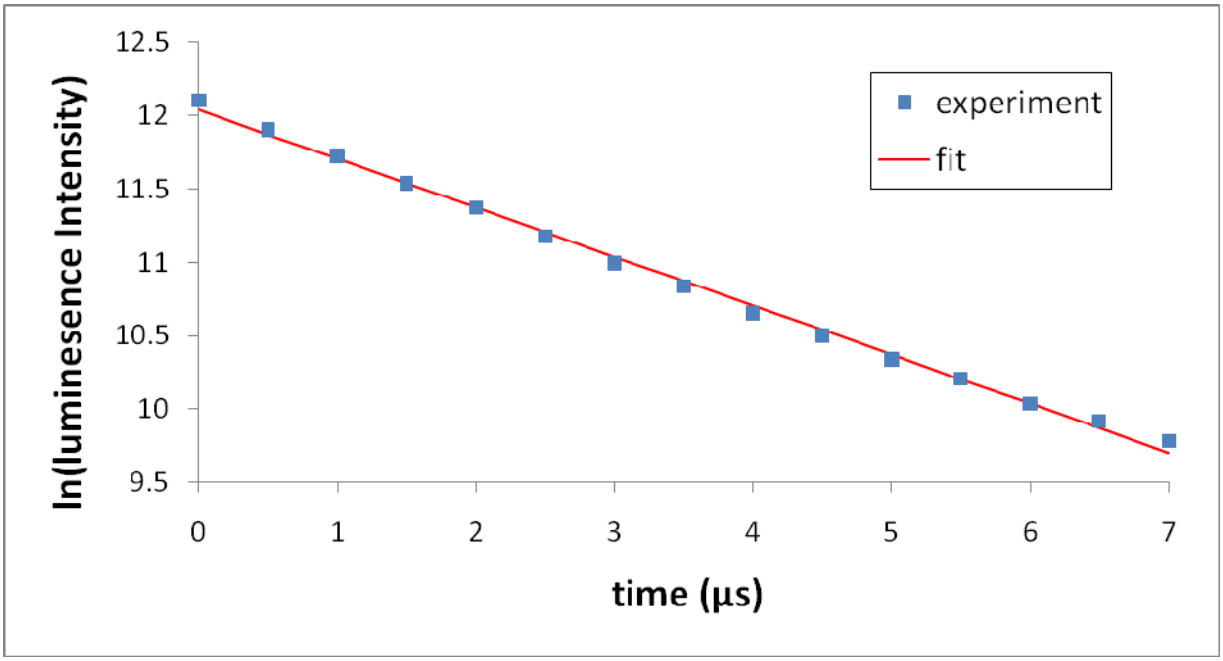

Figure S13. Luminescence decay trace of $(Ph_3P)_2Cu(NTol_2)$ (**2**, λ_{ex} = 337 nm, λ_{em} = 546 nm) with monoexponential fit.

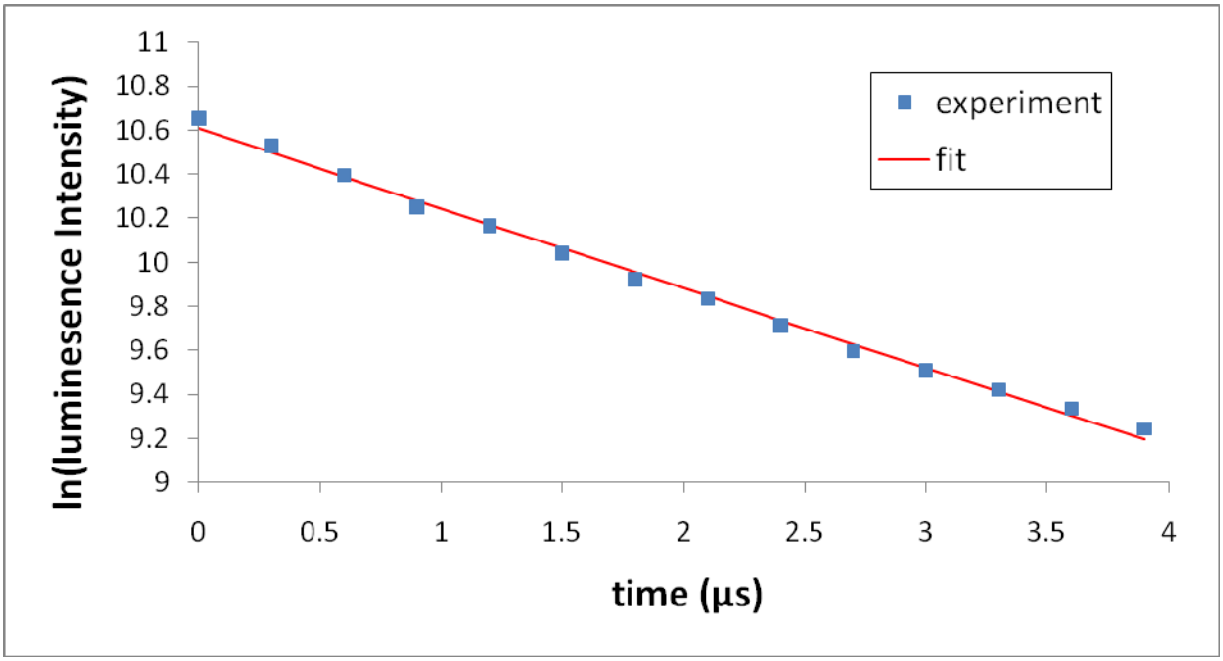

Figure S14. Luminescence decay trace of $(Ph_3P)_2Cu(N(p\text{-}FPh)_2)$ (**3**, λ_{ex} = 337 nm, λ_{em} = 525 nm) with monoexponential fit.

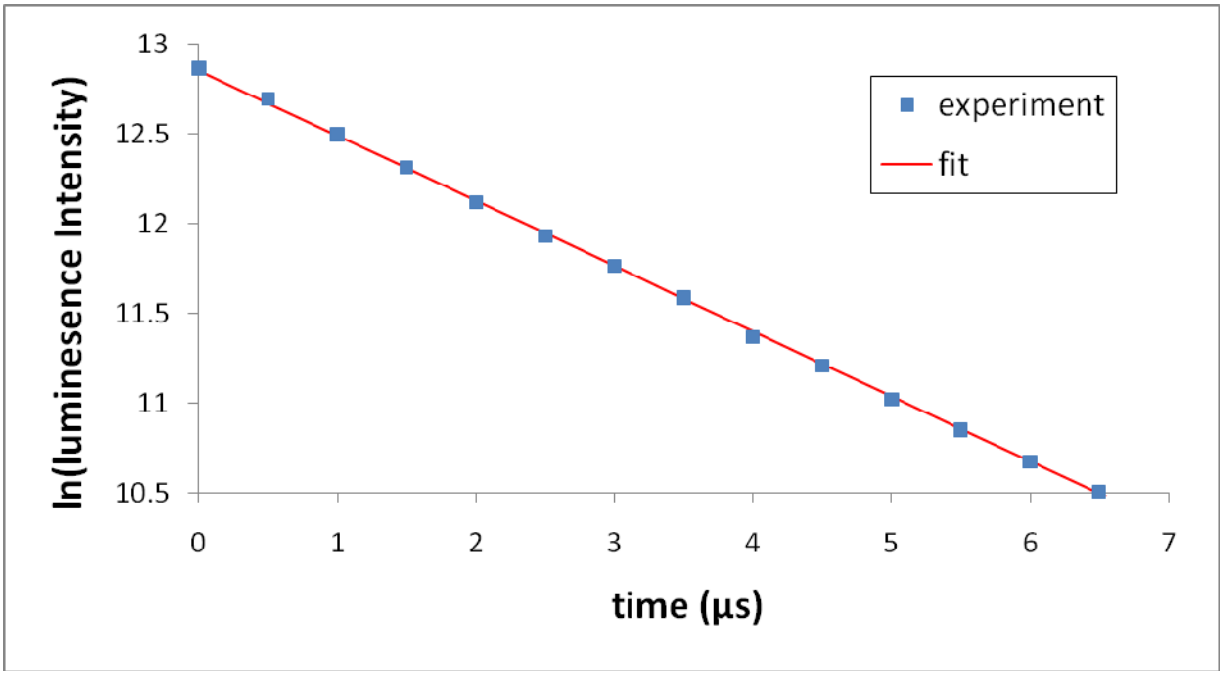

Figure S15. Luminescence decay trace of $(P(p\text{-}Tol)_3)_2Cu(NPh_2)$ (**4**, λ_{ex} = 337 nm, λ_{em} = 509 nm) with monoexponential fit.

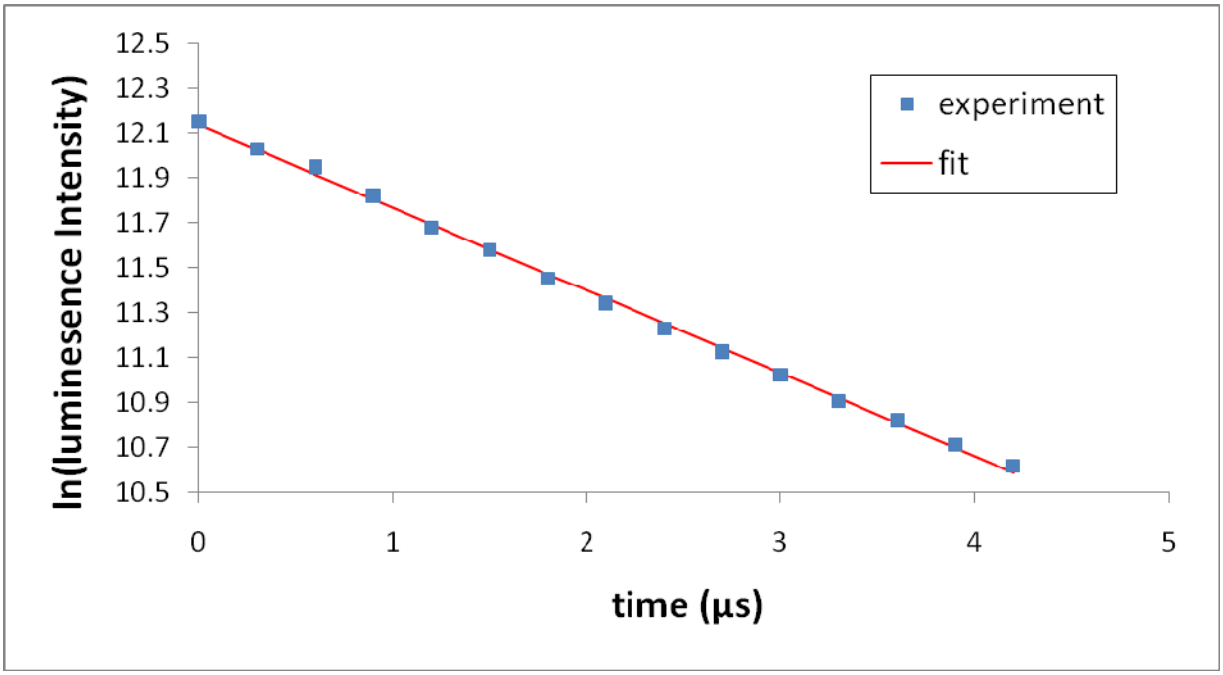

Figure S16. Luminescence decay trace of $(P(p\text{-}FPh)_3)_2Cu(NPh_2)$ (**5**, λ_{ex} = 337 nm, λ_{em} = 535 nm) with monoexponential fit.

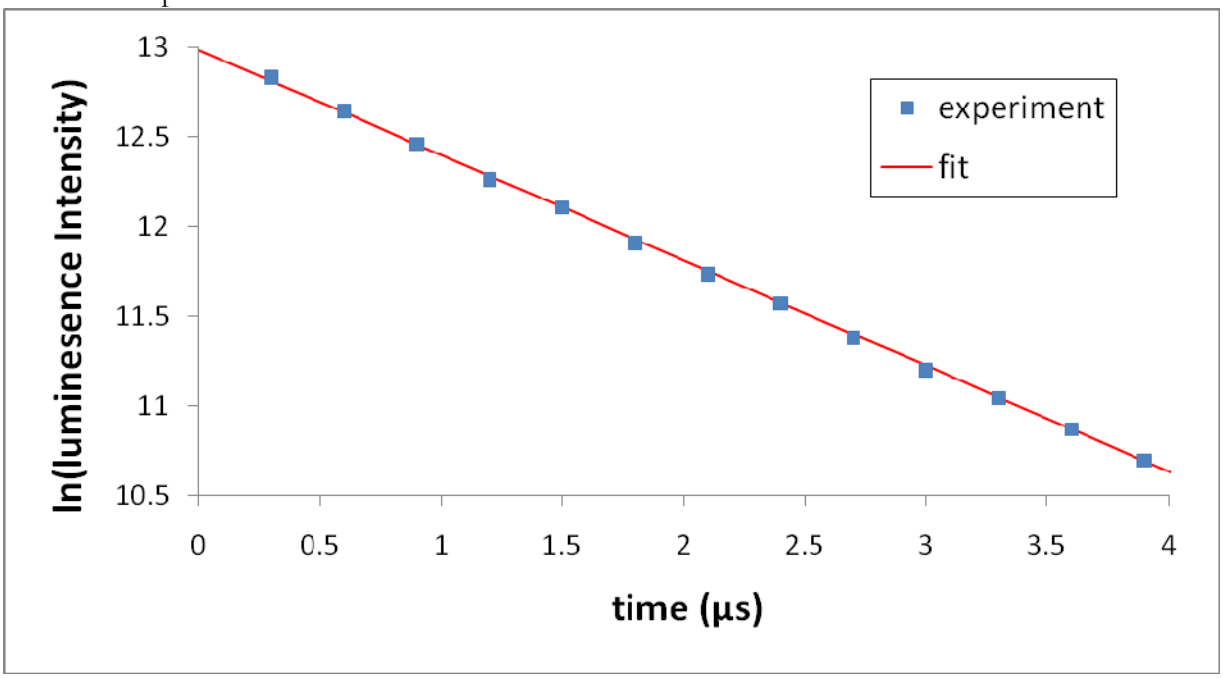

Figure S17. Luminescence decay trace of $(DPEphos)_2Cu(NPh_2)$ (**6**, λ_{ex} = 337 nm, λ_{em} = 563 nm) with monoexponential fit.

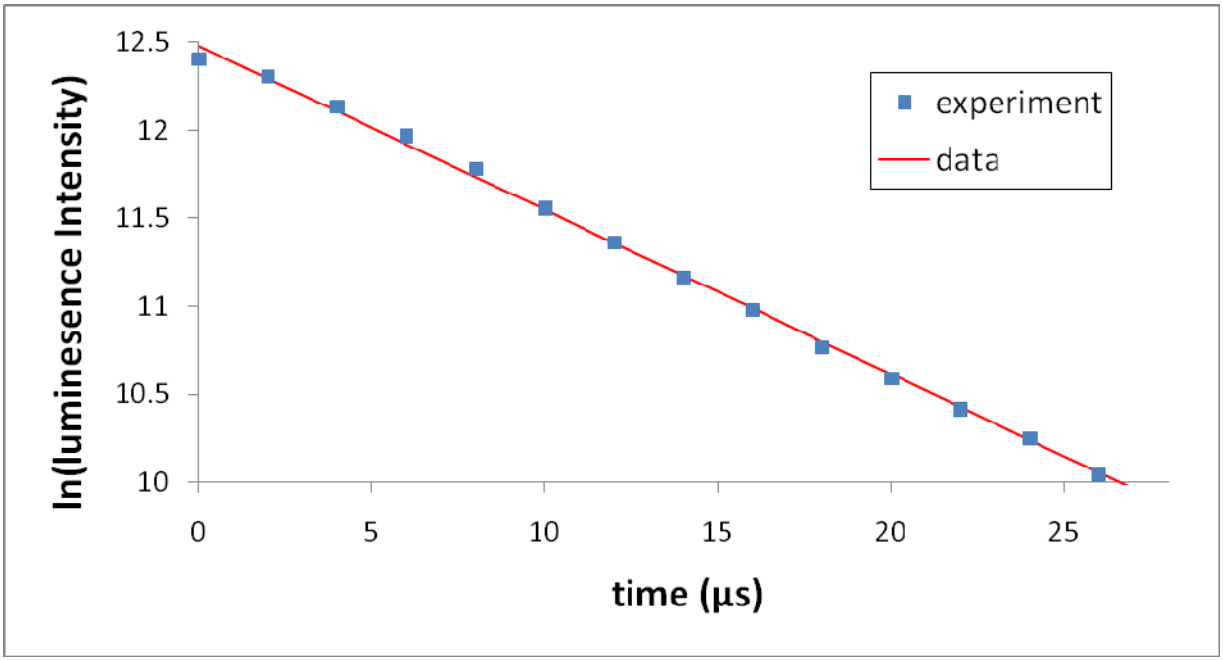

Figure S18. Luminescence decay trace of $(Ph_3P)_2Cu(cbz)$ (**7**, λ_{ex} = 337 nm, λ_{em} = 461 nm) with monoexponential fit.

Table S4. Summary of Crystallographic Data for **1-3,** and **7**.

$(Ph_3P)_2Cu(NPh_2)$ (**1**) CCDC#: 766167	$(Ph_3P)_2Cu(NTol_2)$ (**2**) CCDC#: 766168	$(Ph_3P)_2Cu(N(p\text{-}FPh)_2)$ (**3**) CCDC#: 766169	$(Ph_3P)_2Cu(cbz)$ **(7)** CCDC#: 766170
Crystal system, space group Triclinic, P-1	**Crystal system, space group** Triclinic, P-1	**Crystal system, space group** Monoclinic, $P2_1/c$	**Crystal system, space group** Triclinic, P-1
Chemical Formula, Molecular Weight $C_{48}H_{40}CuNP_2, C_6H_6$ 834.40	**Chemical Formula, Molecular Weight** $C_{50}H_{44}CuNP_2, C_6H_6$ 862.45	**Chemical Formula, Molecular Weight** $C_{48}H_{38}CuF_2NP_2$ 792.27	**Chemical Formula, Molecular Weight** $C_{48}H_{38}CuNP_2$ 754.27
Unit cell dimensions a = 10.9398(10) Å alpha = 78.8570(10)° b = 12.5085(11) Å beta = 80.204(2)° c = 16.1375(15) Å gamma = 82.876(2)°	**Unit cell dimensions** a = 11.887(2) Å alpha = 76.050(3)° b = 12.290(2) Å beta = 83.284(4)° c = 16.185(3) Å gamma = 88.775(3)°	**Unit cell dimensions** a = 11.0998(19) Å alpha = 90° b = 21.800(4) Å beta = 106.574(6)° c = 16.617(4) Å gamma = 90°	**Unit cell dimensions** a = 11.9487(10)Å alpha = 63.1870(10)° b = 13.8065(11) Å beta = 71.7160(10)° c = 13.8302(11) Å gamma = 69.4760(10)°
Volume 2125.5(3) $Å^3$	**Volume** 2279.0(8) A^3	**Volume** 3853.8(13) $Å^3$	**Volume** 1873.7(3) $Å^3$
Z, Calculated density 2, 1.179 Mg/m^3	**Z, Calculated density** 2, 1.257 Mg/m^3	**Z, Calculated density** 4, 1.354 Mg/m^3	**Z, Calculated density** 2, 1.337 Mg/m^3
Temperature 100 K	**Temperature** 100 K	**Temperature** 100 K	**Temperature** 100 K
Absorption coefficient 0.621 mm^{-1}	**Absorption coefficient** 0.588 mm^{-1}	**Absorption coefficient** 0.691 mm^{-1}	**Absorption coefficient** 0.704 mm^{-1}
Theta range for data collection 1.30 to 29.57°	**Theta range for data collection** 1.31 to 27.57°	**Theta range for data collection** 1.58 to 29.15°	**Theta range for data collection** 1.68 to 29.57°.
Limiting indices -15<=h<=15, -17<=k<=17, -22<=l<=22	**Limiting indices** -15<=h<=15, -15<=k<=15, 0<=l<=21	**Limiting indices** -15<=h<=15, -29<=k<=28, -22<=l<=22	**Limiting indices** -16<=h<=16, -19<=k<=19, -19<=l<=19
Reflections collected / unique 52551 / 11890 [R(int) = 0.0470]	**Reflections collected / unique** 10466 / 10466 [R(int) = 0.0000]	**Reflections collected / unique** 83522 / 10382 [R(int) = 0.0648]	**Reflections collected / unique** 49936 / 10471 [R(int) = 0.0357]
Completeness to theta = 29.57 99.6 %	**Completeness to theta = 27.57** 99.2 %	**Completeness to theta = 29.15** 99.9 %	**Completeness to theta = 29.57** 99.6 %
Refinement method Full-matrix least-squares on F^2	**Refinement method** Full-matrix least-squares on F^2	**Refinement method** Full-matrix least-squares on F^2	**Refinement method** Full-matrix least-squares on F^{-2}
Data / restraints / parameters 11890 / 0 / 578	**Data / restraints / parameters** 10466 / 37/ 542	**Data / restraints / parameters** 10382 / 0 / 487	**Data / restraints / parameters** 10471 / 0 / 469
Goodness-of-fit on F^2 1.042	**Goodness-of-fit on F^2** 1.044	**Goodness-of-fit on F^2** 1.029	**Goodness-of-fit on F^2** 1.043
Final R indices [I>2σ (I)] R1 = 0.0399, wR2 = 0.1066	**Final R indices [I>2σ (I)]** R1 = 0.0311, wR2 = 0.0728	**Final R indices [I>2σ (I)]** R1 = 0.0425, wR2 = 0.0990	**Final R indices [I>2σ (I)]** R1 = 0.0311, wR2 = 0.0824
R indices (all data) R1 = 0.0544, wR2 = 0.1155	**R indices (all data)** R1 = 0.0360, wR2 = 0.0754	**R indices (all data)** R1 = 0.0639, wR2 = 0.1115	**R indices (all data)** R1 = 0.0356, wR2 = 0.0859
Largest diff. peak and hole 0.431 and -0.619 e. $Å^3$	**Largest diff. peak and hole** 0.361 and -0.393 e. $Å^3$	**Largest diff. peak and hole** 1.080 and -0.446 e. $Å^3$	**Largest diff. peak and hole** 0.483 and -0.303 e.$Å^3$

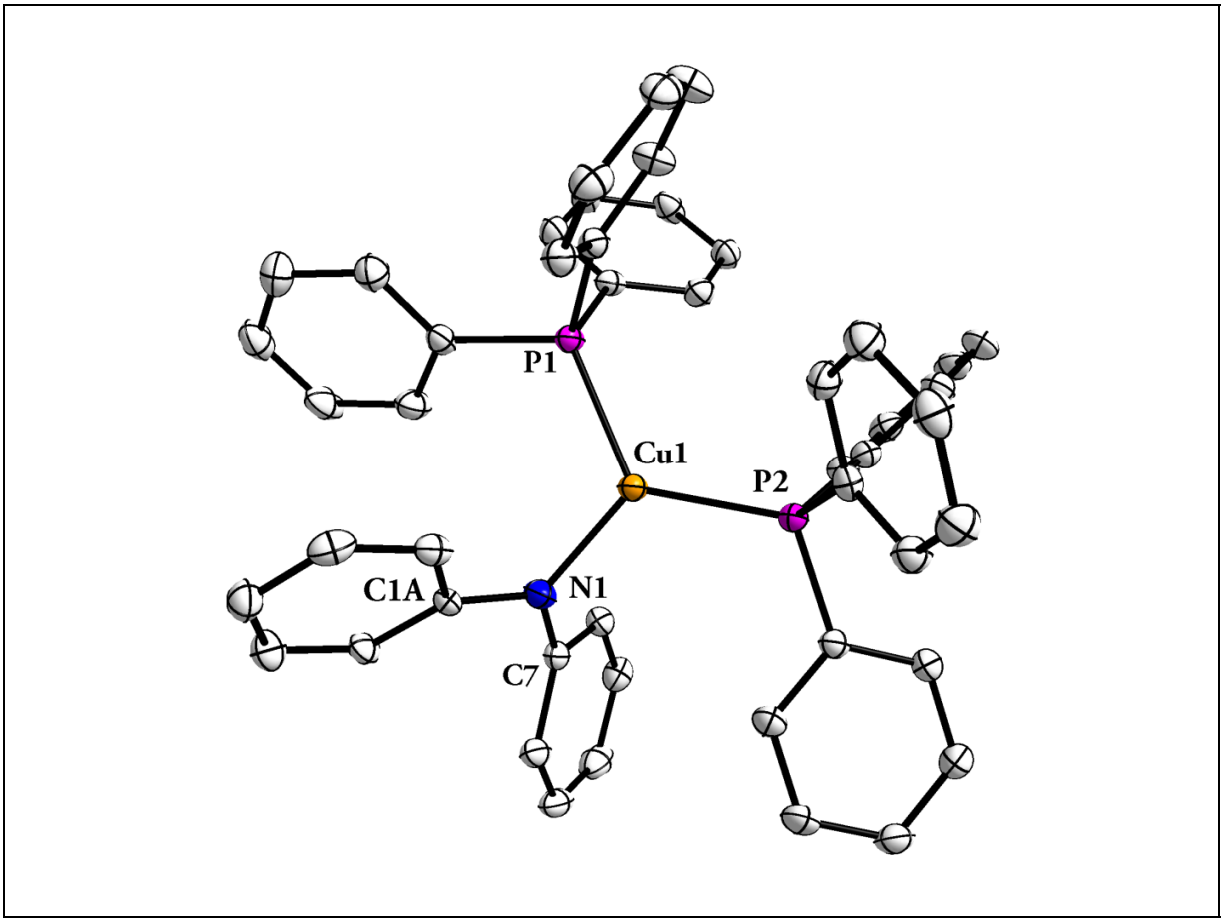

Figure S19. Displacement ellipsoid representation (50%) of $(Ph_3P)_2Cu(NPh_2)$ (**1**). Hydrogen atoms, solvent (benzene), and the minor component of disorder omitted for clarity.

Table S5. Select Bond lengths [Å] and angles [°] for $(Ph_3P)_2Cu(NPh_2)$ (**1**).

Cu(1)-N(1)	1.9602(15)	P(2)-Cu(1)-P(1)	123.995(19)
Cu(1)-P(2)	2.2436(5)	C(1B)-N(1)-C(7)	130.6(10)
Cu(1)-P(1)	2.2598(5)	C(1B)-N(1)-C(1A)	15.7(10)
N(1)-C(1A)	1.411(6)	C(7)-N(1)-C(1A)	117.7(3)
N(1)-C(1B)	1.36(3)	C(1A)-N(1)-Cu(1)	123.5(3)
N(1)-C(7)	1.395(2)	C(1B)-N(1)-Cu(1)	111.2(10)
N(1)-Cu(1)-P(2)	120.72(5)	C(7)-N(1)-Cu(1)	118.14(12)
N(1)-Cu(1)-P(1)	115.29(5)		

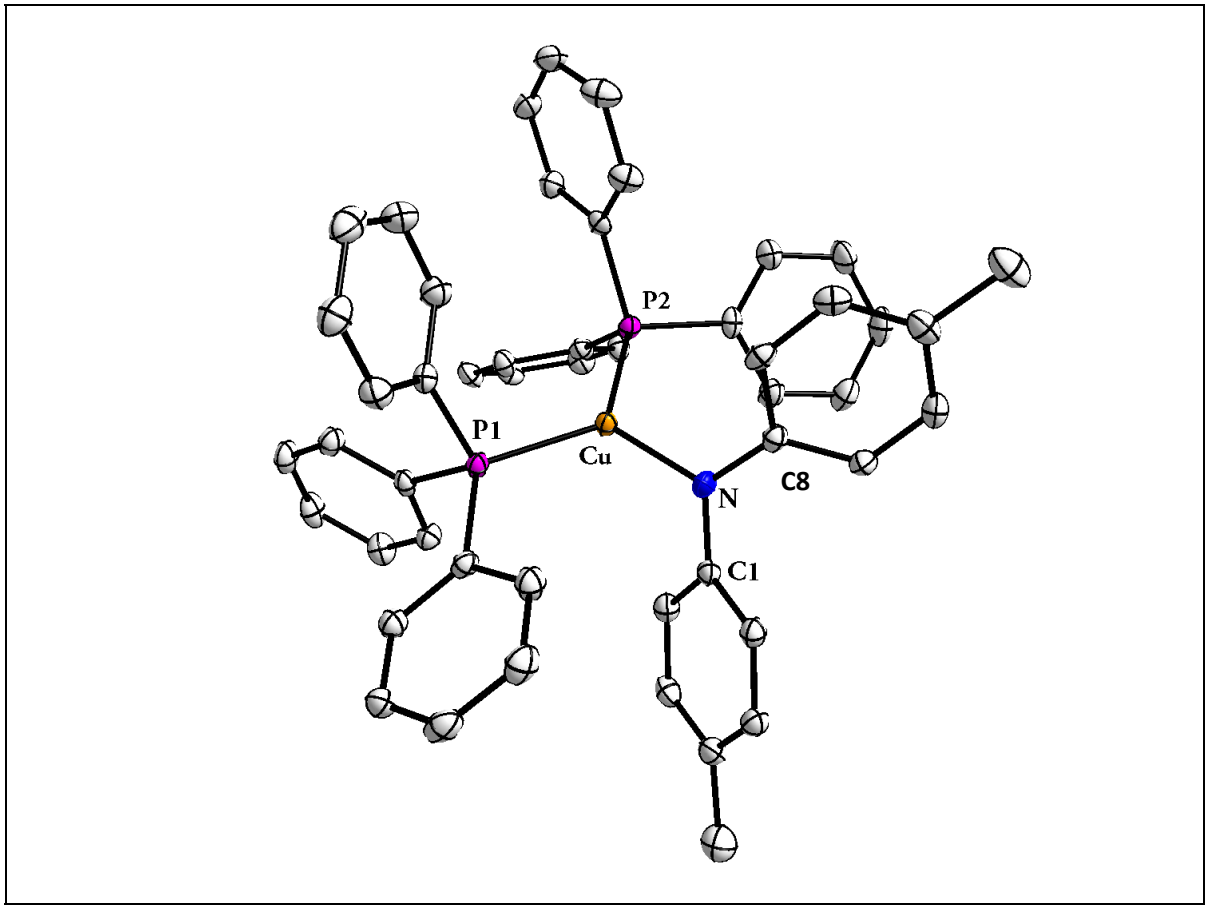

Figure S20. Displacement ellipsoid representation (50%) of $(Ph_3P)_2Cu(NTol_2)$ (**2**). Hydrogen atoms and solvent (benzene) omitted for clarity.

Table S6. Select bond lengths [Å] and angles [°] for $(Ph_3P)_2Cu(NTol_2)$ (**2**).

Cu(1)-N(1)	1.9363(15)	N(1)-Cu(1)-P(2)	117.20(5)
Cu(1)-P(1)	2.2215(6)	P(1)-Cu(1)-P(2)	125.20(2)
Cu(1)-P(2)	2.2357(6)	C(8)-N(1)-C(1)	120.31(14)
N(1)-C(8)	1.389(2)	C(8)-N(1)-Cu(1)	119.53(12)
N(1)-C(1)	1.389(2)	C(1)-N(1)-Cu(1)	120.15(11)
N(1)-Cu(1)-P(1)	117.59(5)		

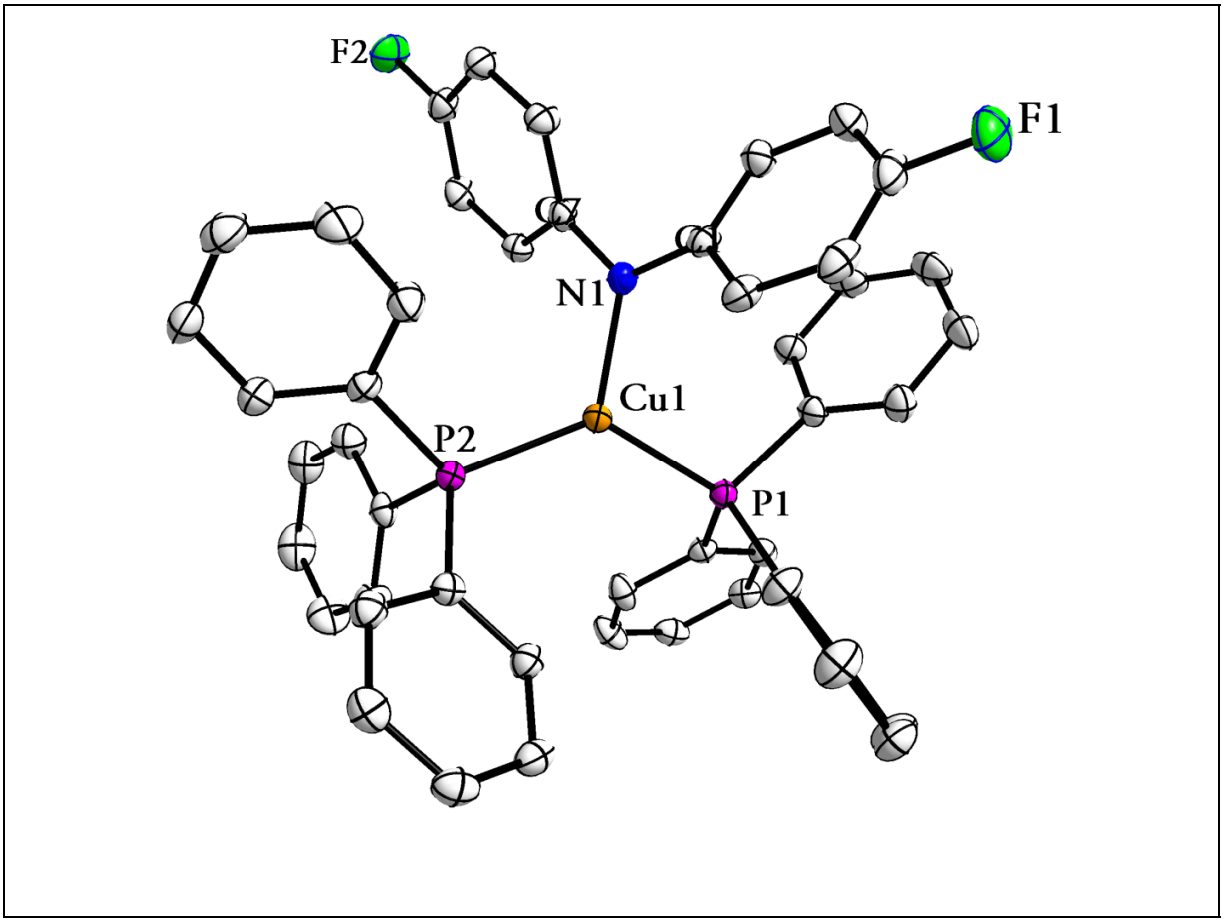

Figure S21. Displacement ellipsoid representation (50%) of $(Ph_3P)_2Cu(N(p\text{-}FPh)_2)$ (**3**). Hydrogen atoms omitted for clarity.

Table S7. Select bond lengths [Å] and angles [°] for $(Ph_3P)_2Cu(N(p\text{-}FPh)_2)$ (**3**).

N(1)-C(7)	1.381(2)	C(7)-N(1)-Cu(1)	121.50(13)
N(1)-C(1)	1.383(2)	C(1)-N(1)-Cu(1)	119.02(13)
N(1)-Cu(1)	1.9547(18)	N(1)-Cu(1)-P(2)	118.88(5)
Cu(1)-P(2)	2.2200(6)	N(1)-Cu(1)-P(1)	111.27(5)
Cu(1)-P(1)	2.2414(6)	P(2)-Cu(1)-P(1)	129.82(2)
C(7)-N(1)-C(1)	119.43(17)		

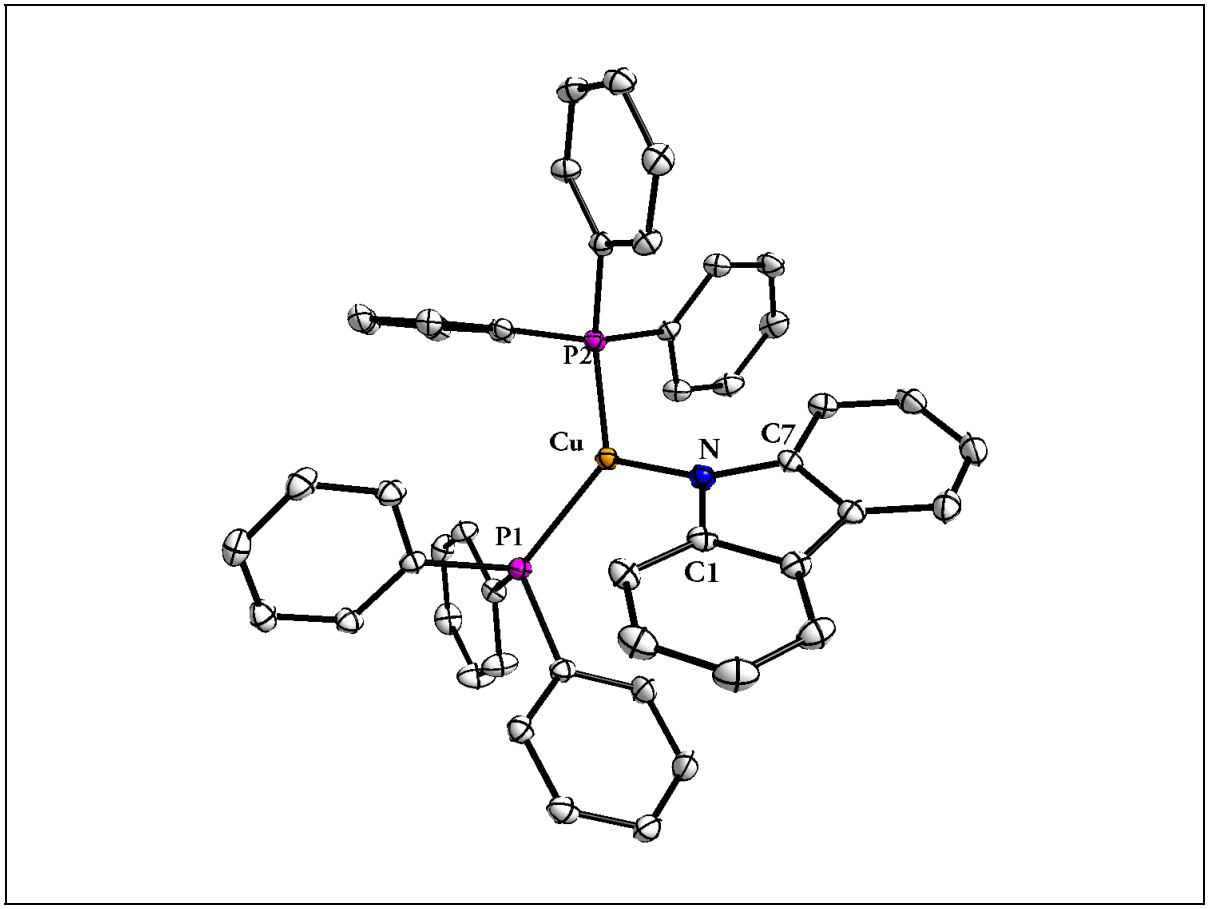

Figure S22. Displacement ellipsoid representation (50%) of $(Ph_3P)_2Cu(cbz)$ (**7**). Hydrogen atoms omitted for clarity.

Table S8. Select bond lengths [Å] and angles [°] for $(Ph_3P)_2Cu(cbz)$ (**7**).

Cu(1)-N(1)	1.9499(11)	N(1)-Cu(1)-P(1)	115.34(3)
Cu(1)-P(2)	2.2467(4)	P(2)-Cu(1)-P(1)	123.616(14)
Cu(1)-P(1)	2.2765(4)	C(7)-N(1)-C(1)	104.97(10)
N(1)-C(7)	1.3869(16)	C(7)-N(1)-Cu(1)	126.98(9)
N(1)-C(1)	1.3913(16)	C(1)-N(1)-Cu(1)	124.93(9)
N(1)-Cu(1)-P(2)	121.05(3)		

References

(1) Fan, L.; Yang, L.; Guo, C.; Foxman, B. M.; Ozerov, O. V. *Organometallics* **2004**, *23*, 4778-4787.
(2) Eriksson, H.; Hkansson, M. *Organometallics*, **1997**, *16*, 4243-4244.
[3] Sheldrick, G. M. *Acta Crystallogr. Sect. A* **1990,** 46, 467.
[4] Sheldrick, G. M. *SHELXL 97;* Universität Göttingen: Göttingen, Germany, 1997.
(5) Müller, P.; Herbst-Irmer, R.; Spek, A. L.; Schneider, T. R.; Sawaya, M. R. *Crystal Structure Refinement: A Crystallographer's Guide to SHELXL*; Oxford University Press: New York, 2003.
(6) Sheldrick, G. M. *Cell_Now*; University of Göttingen, Göttingen, Germany.
(7) Tomas, S. L.; Yagi, S.; Swager, T. M.; *J. Mater. Chem.* **2005**, *15*, 2829-2835.
(8) Demas, J. N.; Crosby, G. A. *J. Phys. Chem.* **1971**, *75*, 991-1024.
(9) Dawson, W. R.; Windsor, M. W. *J. Phys. Chem.* **1968**, *72*, 3251-3260.
(10) Gaussian 03, Revision E.01, Frisch, M. J.; Trucks, G. W.; Schlegel, H. B.; Scuseria, G. E.; Robb, M. A.; Cheeseman, J. R.; Montgomery, Jr., J. A.; Vreven, T.; Kudin, K. N.; Burant, J. C.; Millam, J. M.; Iyengar, S. S.; Tomasi, J.; Barone, V.; Mennucci, B.; Cossi, M.; Scalmani, G.; Rega, N.; Petersson, G. A.; Nakatsuji, H.; Hada, M.; Ehara, M.; Toyota, K.; Fukuda, R.; Hasegawa, J.; Ishida, M.; Nakajima, T.; Honda, Y.; Kitao, O.; Nakai, H.; Klene, M.; Li, X.; Knox, J. E.; Hratchian, H. P.; Cross, J. B.; Bakken, V.; Adamo, C.; Jaramillo, J.; Gomperts, R.; Stratmann, R. E.; Yazyev, O.; Austin, A. J.; Cammi, R.; Pomelli, C.; Ochterski, J. W.; Ayala, P. Y.; Morokuma, K.; Voth, G. A.; Salvador, P.; Dannenberg, J. J.; Zakrzewski, V. G.; Dapprich, S.; Daniels, A. D.; Strain, M. C.; Farkas, O.; Malick, D. K.; Rabuck, A. D.; Raghavachari, K.; Foresman, J. B.; Ortiz, J. V.; Cui, Q.; Baboul, A. G.; Clifford, S.; Cioslowski, J.; Stefanov, B. B.; Liu, G.; Liashenko, A.; Piskorz, P.; Komaromi, I.; Martin, R. L.; Fox, D. J.; Keith, T.; Al-Laham, M. A.; Peng, C. Y.; Nanayakkara, A.; Challacombe, M.; Gill, P. M. W.; Johnson, B.; Chen, W.; Wong, M. W.; Gonzalez, C.; and Pople, J. A.; Gaussian, Inc., Wallingford CT, 2004.
(11) (a) Becke, A. D. *J. Chem. Phys.* **1993**, *98*, 5648-5652. (b) Lee, C.; Yang, W.; Parr, R. G.; *Phys. Rev. B* **1988**, *37*, 785-789.
(12) (a) Rassolov, V. A.; Ratner, M. A.; Pople, J. A.; Redfern , P. C.; Curtiss, L. A. *J. Comp. Chem.*, **22** (2001) 976-84. (b) Rassolov, V. A.; Ratner, M. A.; Pople, J. A.; and Windus , T. L.; *J. Chem. Phys.*, **109** (1998) 1223-29.